Why does steady-state magnetic reconnection have a maximum local rate of order 0.1?

Yi-Hsin Liu,[1] M. Hesse,[1] F. Guo,[2] W. Daughton,[2] H. Li,[2] P. A. Cassak,[3] and M. A. Shay[4]

[1] *NASA-Goddard Space Flight Center, Greenbelt, MD 20771*
[2] *Los Alamos National Laboratory, Los Alamos, NM 87545*
[3] *West Virginia University, Morgantown, WV 26506*
[4] *University of Delaware, Newark, DE 19716*

(Dated: November 24, 2016)

Simulations suggest collisionless steady-state magnetic reconnection of Harris-type current sheets proceeds with a rate of order 0.1, independent of dissipation mechanism. We argue this long-standing puzzle is a result of constraints at the magnetohydrodynamic (MHD) scale. We perform a scaling analysis of the reconnection rate as a function of the opening angle made by the upstream magnetic fields, finding a maximum reconnection rate close to 0.2. The predictions compare favorably to particle-in-cell simulations of relativistic electron-positron and non-relativistic electron-proton reconnection. The fact that simulated reconnection rates are close to the predicted maximum suggests reconnection proceeds near the most efficient state allowed at the MHD-scale. The rate near the maximum is relatively insensitive to the opening angle, potentially explaining why reconnection has a similar fast rate in differing models.

PACS numbers: 52.35.Vd, 94.30.cp, 96.60.Iv

arXiv:1611.07859v1 [physics.plasm-ph] 23 Nov 2016

Introduction– Magnetic energy is abruptly released in solar and stellar flares [1–3], substorms in magnetotails of Earth and other planets [4, 5], disruptions and the sawtooth crash in magnetically confined fusion devices [6], laboratory experiments [7], and numerous high energy astrophysical systems [8, 9]. Magnetic reconnection, where a change in topology of the magnetic field allows a rapid release of magnetic energy into thermal and kinetic energy, is a likely cause. The reconnection electric field parallel to the X-line (where magnetic field lines break) not only determines the rate that reconnection proceeds, but can also be crucial for accelerating energetic superthermal particles. It was estimated that a normalized reconnection rate of $\simeq 0.1$ is required to explain time scales of flares and substorms [10].

Reconnection rates have been studied observationally, experimentally, theoretically, and numerically. Measurements can be *in situ*, such as in the magnetosphere and lab, or remote, as in solar and astrophysical contexts. Reconnection rates from these different vantage points can be the same but need not be; for example, flux ropes in the corona have macroscopic forces that can influence the evolution of current sheets where reconnection occurs. Therefore, it is important to distinguish between system scales. We define *global-scale* as system-size scale of magnetic domains. The *local-scale* is a smaller MHD-scale region where the magnetic field and plasma parameters achieve relatively uniform conditions upstream of the diffusion region. The *micro-scale* is the scale of the diffusion region. Here we focus on reconnection rates at the local- and micro-scales; coupling to global scales is beyond the scope of this paper.

The original model for the *local* reconnection rate was the Sweet-Parker model [11, 12], but it was too slow to explain observed time scales of flares and substorms [13]. The collisional diffusion region is long and thin (*i.e.,* the upstream magnetic fields have a small opening angle), developing a bottleneck that keeps the inflow speed small. The Petschek model [14] was much faster by producing an open outflow region (*i.e.,* a larger opening angle), but is not a self-consistent model [15, 16].

The collisionless limit is more appropriate for many systems of interest. Two-dimensional (2D) local simulations of isolated, thin, Harris-type current sheets reveal that the steady-state reconnection has a fast rate of 0.1 [17] when normalized by the magnetic field and Alfvén speed at the local-scale. This rate is independent of simulated electron mass [18, 19] and system size [17, 19]. In particular, the GEM challenge study [20] showed that the rate is comparable in Hall-MHD, hybrid, and particle-in-cell (PIC) simulations. Consequently, it was argued that the Hall term, the minimal non-ideal-MHD term in all three models, is the key physics for producing the fast rate [21, 22]. However, further studies have raised important questions. One gets similar fast rates in electron-positron plasmas, for which the Hall term vanishes [23–25], and in the strong out-of-plane (guide) magnetic field regime [26–29] for which the Hall term is inactive. Even within resistive-MHD, the same 0.1 rate arises when a localized resistivity is employed [16]. This evidence calls into question whether the Hall term is the critical effect. It was suggested that the appearance of secondary islands could provide a universal mechanism for limiting the length of the diffusion region [24, 26], but this model is also not satisfying since the same rate is obtained even when islands are absent [22, 30].

In situ magnetospheric observations reveal (local) reconnection rates near 0.1 [31, 32]. Solar observations suggest (global) reconnection rates can be this high as well [33–35], or somewhat lower [36, 37]. Therefore, ob-

servations suggest the *local* rate is 0.1, and the *global* rate can be at or below 0.1. This also has numerical support; in island coalescence, the *global* rate can be lower than 0.1 [38–40], while the *local* rate remains close to 0.1 [38].

What causes the *local* reconnection rate to be ~ 0.1 across different systems remains an open question [e.g., Ref. [41]]. In this paper, we offer a new approach to this long-standing problem. We propose that the *local* rate has a maximum as a result of constraints at MHD scales (rather than physics at the diffusion-region-scale as is typically discussed). We perform a scaling analysis to derive the maximum *local* rate for low-β plasmas, which we find is $O(0.1)$. The fact that local simulations produce rates close to this maximum value suggests that steady reconnection proceeds at a rate nearly as fast as possible. We show the predictions are consistent with PIC simulations of a relativistic electron-positron plasma and a non-relativistic electron-proton plasma.

Simple model– Let the thickness and length of the (micro-scale) diffusion region be δ and L, respectively. For collisionless reconnection, δ is controlled by inertial or gyro-radius scales [42]. If the opening angle made by the upstream magnetic field is small, the diffusion region is long and thin. Reconnection in this case is very slow, as in Sweet-Parker reconnection [11, 12]. As the opening angle increases, reconnection becomes faster. This is true to a point, but cannot continue for all angles for two reasons. First, in order to satisfy force balance, the upstream region develops structures over a larger scale, as in the classical Petschek-type analyses [14, 43]; this is what we define as the local-scale. Since the diffusion region thickness continues to be controlled by micro-scales, the diffusion region becomes embedded in a wider structure [42, 44, 45] of local-scale Δz, where the magnetic field and plasma parameters achieve relatively uniform upstream conditions. The magnetic field B_{xm} immediately upstream of the diffusion region becomes smaller than the asymptotic magnetic field B_{x0}. (The subscript "0" indicates asymptotic quantities at the *local-scale* and "m" indicates quantities at the *micro-scale*.) This is crucial because it is B_{xm} that drives the outflow from the diffusion region; as it becomes smaller, reconnection proceeds more slowly.

The second reason reconnection does not become faster without bound is that the $\mathbf{J}\times\mathbf{B}$ force of the reconnected field becomes smaller as the opening angle increases [46]. In the limit where the separatrices are at a right angle, the tension force driving the outflow is canceled by the magnetic pressure force, so reconnection does not spontaneously occur.

These observations suggest the following: the reconnection rate has a maximal value for an intermediate opening angle which is large enough to avoid the bottleneck for extremely thin current layers, but is not too large to weaken the reconnection drive. We present a scaling analysis simply capturing these main aspects using

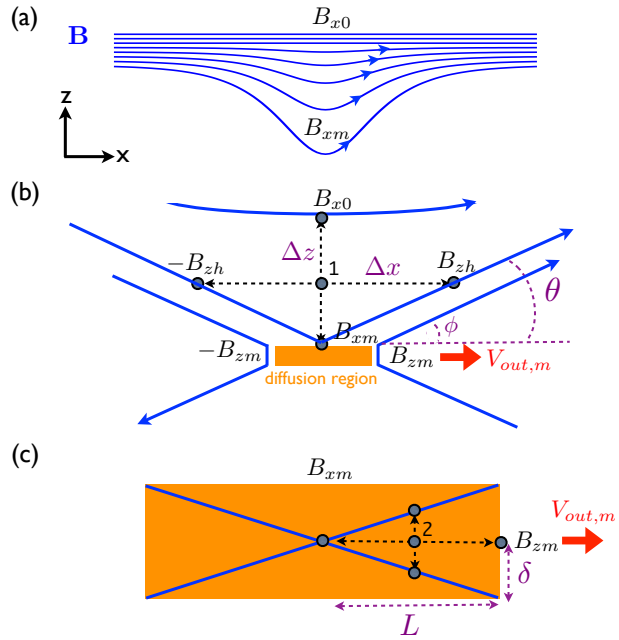

FIG. 1: (a) Sketch of magnetic field lines upstream of the diffusion region ($z > 0$). (b) Geometry of reconnection at the local-scale. (c) Dimensions of the diffusion region at the micro-scale.

only the reconnection geometry and force balance. We consider low-β systems in the relativistic limit; a more general derivation should be future work.

The inflow region is illustrated in Fig. 1(a). With the diffusion region at the micro-scale, the asymptotic (local) magnetic field (at the top) must bend as it weakens toward the diffusion region (at the bottom). In the $\beta \ll 1$ limit, thermal pressure is negligible, so to remain near equilibrium the inward-directed magnetic pressure gradient force $-(\nabla B^2/8\pi)_z$ must be almost perfectly balanced by outward-directed magnetic tension $\mathbf{B}\cdot\nabla B_z/4\pi$. Evaluating these at point 1 marked in Fig. 1(b) gives

$$\frac{B_{x0}^2 - B_{xm}^2}{8\pi\Delta z} \simeq \left(\frac{B_{x0}+B_{xm}}{2}\right)\frac{2B_{zh}}{4\pi\Delta x}, \tag{1}$$

where B_{zh} is evaluated at the upstream field line near the separatrix.

We make the reasonable assumption the opening angle made by the upstream field at the local-scale, $\theta \equiv \tan^{-1}(\Delta z/\Delta x)$, matches the opening angle of the micro-scale field at the corner of the diffusion region, $\phi \equiv \tan^{-1}(B_{zm}/B_{xm})$. Then, from geometry, we get $B_{zh}/[(B_{x0}+B_{xm})/2] \simeq \Delta z/\Delta x \simeq B_{zm}/B_{xm}$. Eliminating B_{zh} and solving for B_{xm}/B_{x0} gives

$$\frac{B_{xm}}{B_{x0}} \simeq \frac{1-(\Delta z/\Delta x)^2}{1+(\Delta z/\Delta x)^2}. \tag{2}$$

For small opening angles, $B_{xm} \simeq B_{x0}$; for large opening angles approaching 45°, $B_{xm} \ll B_{x0}$, and embedding is significant.

To estimate the outflow speed, we employ force balance in the x-direction at point 2 in Fig. 1(c). In the relativistic limit [47], $n' m_i U_{out}^2/2L + B_{zm}^2/8\pi L \simeq (B_{zm}/2)2(B_{xm}/2)/4\pi\delta$, where n' is the density measured in the fluid rest frame, m_i is the ion mass, U_{out} is the x-component of the 4-velocity. Note that we have assumed that the profile of plasma pressure in the outflow direction is nearly uniform, as has been done in previous analyses [48], so that the pressure gradient force is small compared to the magnetic tension force. The outflow speed $V_{out,m}$ from the end of the diffusion region is related to U_{out} through $U_{out} = \gamma_{out} V_{out,m} = V_{out,m}/(1 - V_{out,m}^2/c^2)^{1/2}$, where γ_{out} is the relativistic factor. Since the separatrix goes through the corner of the diffusion region, $B_{zm}/B_{xm} \simeq \delta/L$. Solving for the outflow speed as a function of δ/L gives

$$V_{out,m} \simeq c\sqrt{\frac{(1-\delta^2/L^2)\sigma_{xm}}{1+(1-\delta^2/L^2)\sigma_{xm}}}, \tag{3}$$

where the magnetization parameter evaluated near the diffusion region is $\sigma_{xm} = B_{xm}^2/4\pi n' m_i c^2$. Consequently, if $\delta/L \ll 1$, then $V_{out,m} \sim V_{Am}$ as expected since the Alfvén speed in the relativistic limit [49] is $V_{Am} = c[\sigma_{xm}/(1+\sigma_{xm})]^{0.5}$. However, as $\delta/L \to 1$, the outflow speed $\to 0$ [46].

Putting the results together yields a prediction for the normalized *local* rate. The reconnection electric field E_y is $B_{zm} V_{out,m}/c$. The reconnection rate $R_0 \equiv cE_y/B_{x0}V_{A0}$ normalized to local quantities is

$$R_0 \simeq \left(\frac{B_{zm}}{B_{xm}}\right)\left(\frac{B_{xm}}{B_{x0}}\right)\left(\frac{V_{out,m}}{V_{A0}}\right). \tag{4}$$

The rate normalized to the micro-scale magnetic field and Alfvén speed is $R_m \simeq (B_{zm}/B_{xm})(V_{out,m}/V_{Am})$, and the micro-scale inflow speed is $V_{in,m} \simeq R_m V_{Am}$.

Writing Eqs. (2) and (3) as functions of $\Delta z/\Delta x$ and substituting into Eq. (4) gives the predicted *local* rate. In the non-relativistic limit ($\sigma_{x0} \ll 1$), the rate is

$$R_{0,NR} \simeq \frac{\Delta z}{\Delta x}\left[\frac{1-(\Delta z/\Delta x)^2}{1+(\Delta z/\Delta x)^2}\right]^2 \sqrt{1-\left(\frac{\Delta z}{\Delta x}\right)^2}, \tag{5}$$

which is plotted as the solid curve in Fig. 2(a). This expression generalizes the previously known result [11, 12, 46] of $R_{0,NR} \simeq \Delta z/\Delta x \simeq \delta/L$ for small opening angles. In the $\Delta z/\Delta x \to 0$ and $\Delta z/\Delta x \to 1$ limits, $R_{0,NR}$ vanishes. Between the two extremes, $R_{0,NR}$ has a maximum, conforming to the discussion earlier. The maximum occurs at $\Delta z/\Delta x \simeq 0.31$ corresponding to a rate of 0.2, close to the fast rate of order 0.1 widely observed. More importantly, the *local* rate is relatively flat for a broad range of $\Delta z/\Delta x$ around the optimal value, suggesting that the rate is not strongly sensitive to the opening angle for intermediate values. This may explain why reconnection rates in disparate physical systems are so similar.

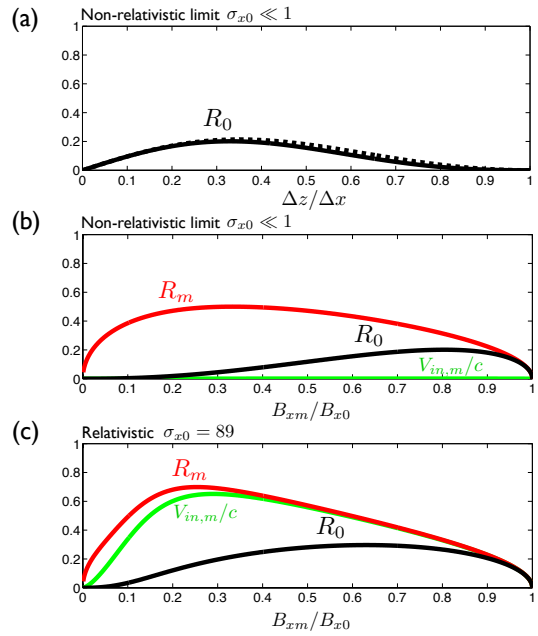

FIG. 2: Predictions for the non-relativistic limit as functions of (a) $\Delta z/\Delta x$ and (b) B_{xm}/B_{x0}. (c) Predictions for relativistic limit ($\sigma_{x0} = 89$).

The dotted curve in Fig. 2(a) shows the non-relativistic prediction if $V_{out,m}$ is taken to be identically V_{Am} in Eq. (4). This comparison indicates that the correction to the outflow speed in Eq. (3) does not significantly alter R_0, although it does impact R_m as $\Delta z/\Delta x$ approaches 1. Thus, the most significant effect limiting the *local* rate with a increasing opening angle is the embedding. We plot R_0, R_m and $V_{in,m}/c$ in Fig. 2(b) as functions of B_{xm}/B_{x0} to facilitate a comparison with simulations. A similar plot is shown in Fig. 2(c) for the relativistic limit, specifically with $\sigma_{x0} = 89$. The peak R_0 is 0.3, and it does not change with increasing σ_{x0}. This bounds rates seen in relativistic simulations [45, 50–53].

We point out that there are similarities between the present model and the classical Petschek model [14]. However, there are a number of important differences. For example, the Petschek model assumes a value of 0.5 for what we call B_{xm}/B_{x0}, whereas we estimate it self-consistently. Furthermore, the way Petschek obtained the upstream condition, strictly speaking, only works for the small opening angle limit, while our result is valid for any opening angle. Finally, and most importantly, the weak dependence on reconnection rate reported by Petschek has a logarithmic dependence on Lundquist number, so the normalized reconnection rate is not bounded by 0 and 1 as it must be on physical grounds. In the present work, the reconnection rate is manifestly bounded between 0 and 1.

Comparison to particle-in-cell simulations– We com-

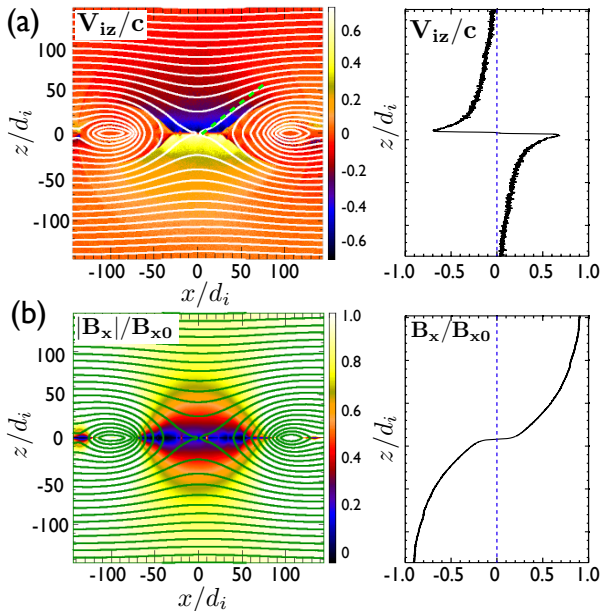

FIG. 3: Local-scale structure around the X-line in electron-positron reconnection with $\sigma_{x0} = 89$ at $t = 600/\omega_{pi}$. (a) V_{iz} and its cut at $x = 0$. (b) $|B_x|$ and a cut of B_x at $x = 0$. Contours of in-plane magnetic flux are overlaid. The color table in (b) has an upper limit B_{x0}.

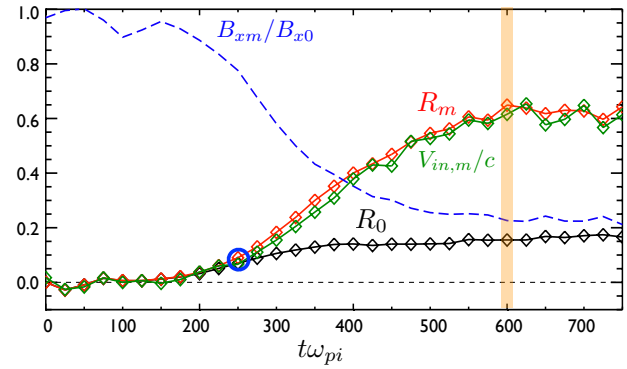

FIG. 4: Time evolution of the measured local reconnection rate R_0, micro-scale rate R_m, micro-scale inflow speed $V_{in,m}/c$ and B_{xm}/B_{x0}. The blue circle marks the deviation of R_m from R_0. The orange vertical line marks the time plotted in Fig. 3.

pare the predictions against PIC simulations of a relativistic electron-positron plasma (*i.e.*, $m_i = m_e$) in Ref. [45]. The upstream magnetization parameter $\sigma_{x0} = 89$ and $\beta = 0.005$. The diffusion region is embedded, as is clearly seen in Fig. 3 which shows the inflow velocity V_{iz} and reconnecting magnetic field B_x with in-plane magnetic flux overlaid at time $t = 600/\omega_{pi}$. A vertical cut through the X-line of these quantities is also shown. Immediately upstream of the diffusion region of d_i-scale thickness, $|V_{iz}|$ peaks at $\simeq 0.65c$ and $|B_x|/B_{x0}$ drops to $\simeq 0.2$ ($d_i = c/\omega_{pi}$ is the ion inertial scale). The variation of the magnetic structure extends $\gtrsim 100d_i$ upstream, and the separatrix has an opening angle wider than typically seen in the non-relativistic regime with $\beta \sim O(1)$ (*e.g.*, [18]). It was shown in Ref. [45] that the magnetic pressure gradient balances magnetic tension in the upstream region, as expected for this low-β system.

The time evolution of reconnection rates are plotted in Fig. 4, along with the micro-scale inflow speed $V_{in,m}$ and the ratio of magnetic fields B_{xm}/B_{x0}. Before a quasi-steady state is reached, both R_m and R_0 increase as the simulation progresses. The deviation of R_m from R_0 occurs at time $t \simeq 250/\omega_{pi}$ and $B_{xm}/B_{x0} \simeq 0.8$. R_0 reaches a plateau of $\simeq 0.15$ at $t \gtrsim 300/\omega_{pi}$ while R_m continues to grow and B_{xm}/B_{x0} continues to drop. Note that, $R_0 \simeq 0.15$ is reached before the generation of secondary tearing modes at $t \simeq 500/\omega_{pi}$, indicating that R_0 is not determined by secondary islands. R_m eventually reaches a plateau of $\simeq 0.6$ and B_{xm}/B_{x0} drops to $\simeq 0.22$ at $t \gtrsim 600/\omega_{pi}$. The inflow speed $V_{in,m}$ traces R_m because $V_{Am} \simeq c$. We compare the steady-state values to the prediction shown in Fig. 2(c). Substituting the measured $B_{xm}/B_{x0} \simeq 0.22$ into the predictions gives $R_0 \simeq 0.14$, $R_m \simeq 0.69$, $V_{in,m} \simeq 0.62c$ and an opening angle $\theta \simeq 38.7°$ [illustrated by the dashed green line in Fig. 3(a)]. Given the simplicity of this model, this agreement is quite remarkable.

To test the predictions against non-relativistic electron-proton reconnection, we compare with a low-β PIC simulation in Ref. [54], which used $m_i/m_e = 25$ and a background density 1% of the sheet density. The upstream $\beta = 0.01$. From that reference, $R_0 \simeq 0.085$ and $R_m \simeq 0.22$ with $B_{xm}/B_{x0} \simeq 0.55$. The predictions in Fig. 2(b) based on $B_{xm}/B_{x0} \simeq 0.55$ are roughly twice these values, mainly because of an overestimation of the outflow speed. However, it is common for electron-proton plasmas to have outflow speeds about half of the Alfvén speed [54]; this is likely due to a self-generated firehose-sense temperature anisotropy in reconnection exhausts, which reduces the outflow speed (*e.g.*, [55, 56]) but is not considered in the current model. Adjusting for this factor of two, the predictions agree quite well with the simulations. The predicted opening angle $\sim 28.8°$ purely based on the upstream constraint in Eq. (2) agrees well.

Discussion– The model presented here is completely independent of dissipation mechanism. The only ingredients are MHD-scale considerations and that the diffusion region remains at micro-scales when the opening angle increases. The fact that the simulated fast rates in disparate physical models are all similar to the predicted maximum rate of order 0.1 suggests that MHD-scale constraints on magnetic energy release determine the fast rate. The obvious counterpoint to this is reconnection in MHD simulations with a uniform resistivity, which does not proceed at this rate. Even when the Lundquist number is large enough to produce magnetic

islands [15, 57], the reconnection rate is an order of magnitude smaller [58–60]. This indicates that considerations at MHD scales are not sufficient to explain fast reconnection; the micro-scale dissipation/localization mechanism must be able to support the desired opening angle at the local-scale. However, if the diffusion region can support a larger opening angle, the *local* rate of order $\sim O(0.1)$ is not strongly sensitive to the opening angle over a wide range of values. The micro-scale rate R_m is sensitive to the opening angle, resulting in the large difference between R_m and R_0 observed in the relativistic limit [45].

The present model is not complete in that it does not include some physics that may affect the reconnection rate. As discussed earlier, the self-generated pressure anisotropy in the exhaust can reduce the outflow speed [55, 56]. The plasma pressure gradient force in the outflow direction can also affect the outflow speed [26, 54, 61]. Self-generated upstream temperature anisotropies [62] may modify the embedding. Relaxing the low-β assumption is important. However, we note that the reduction of B_{xm} also occurs in simulations with $\beta \sim O(1)$ in Ref. [54]. Finally, this model does not take into account the conversion of upstream energy into heat and accelerated particles, which undoubtedly impacts the energy conversion process and is important in maintaining the intense current sheet during reconnection [46, 63]. Nevertheless, this simple model offers a new approach to the long-standing fast reconnection rate problem, which is broadly relevant in basic plasma physics, fusion science, solar and space physics, and astrophysics, and potentially provides an avenue for understanding the important link between the micro- and global-scales.

Y.-H. Liu thanks M. Swisdak and J. C. Dorelli for helpful discussions, and P. Wu for sharing her simulation data. Y.-H. Liu is supported by NASA grant NNX16AG75G. M. Hesse acknowledges support by NASA's MMS mission. F. Guo is supported by NASA grant NNH16AC601. H. Li is is supported by the DOE through the LDRD program at LANL and DOE/OFES support to LANL in collaboration with CMSO. P. A. Cassak acknowledges support from NSF Grants AGS-0953463 and AGS-1460037 and NASA Grants NNX16AF75G and NNX16AG76G. M. Shay is supported by NSF grant AGS-1219382. Simulations were performed with LANL institutional computing, NASA Advanced Supercomputing and NERSC Advanced Supercomputing.

[1] S. Masuda, T. Kosugi, H. Hara, S. Tsuneta, and Y. Ogawara, Nature **371**, 495 (1994).
[2] R. E. Gershberg, *Solar-Type Activity in Main-Sequence Stars* (Springer, Berlin, 2005).
[3] J. A. Klimchuk, Phil. Trans. R. Soc. A **373**, 20140256 (2015).
[4] L. Kepko, R. L. McPherron, O. Amm, S. Apatenkov, W. Baumjohann, J. Birn, M. Lester, R. Nakamura, T. I. Pulkkinen, and V. Sergeev, Space Sci Rev **190**, 1 (2015).
[5] V. M. Vasyliunas, *Plasma distribution and flow* (edited by A. J. Dessler, Cambridge Univ. Press, Cambridge, UK, 1983), chap. 395.
[6] M. Yamada, F. M. Levinton, N. Pomphrey, R. Budny, J. Manickam, and Y. Nagayama, Phys. Plasmas **1**, 3269 (1994).
[7] M. Yamada, Y. Ren, H. Ji, J. Breslau, S. Gerhardt, R. Kulsrud, and A. Kuritsyn, Phys. Plasmas **13**, 052119 (2006).
[8] L. Sironi, M. Petropoulou, and D. Giannios, MNRAS **450**, 183 (2015).
[9] E. G. Zweibel and M. Yamada, ARA&A **47**, 291 (2009).
[10] E. N. Parker, Ap. J. **180**, 247 (1973).
[11] P. A. Sweet, in *IAU Symp. in Electromagnetic Phenomena in Cosmical Physics, ed. B. Lehnet (New York: Cambridge Univ. Press)* (1958), p. 123.
[12] E. N. Parker, J. Geophys. Res. **62**, 509 (1957).
[13] E. N. Parker, Astrophys. J. **8**, 177 (1963).
[14] H. E. Petschek, in *Proc. AAS-NASA Symp. Phys. Solar Flares* (1964), vol. 50 of *NASA-SP*, pp. 425–439.
[15] D. Biskamp, Phys. Fluids **29**, 1520 (1986).
[16] T. Sato and T. Hayashi, Phys. Fluids **22**, 1189 (1979).
[17] M. A. Shay, J. F. Drake, B. N. Rogers, and R. E. Denton, Geophys. Res. Lett. **26**, 2163 (1999).
[18] M. A. Shay and J. F. Drake, Geophys. Res. Lett. **25**, 3759 (1998).
[19] M. Hesse, K. Schindler, J. Birn, and M. Kuznetsova, Phys. Plasmas **6**, 1781 (1999).
[20] J. Birn, J. F. Drake, M. A. Shay, B. N. Rogers, R. E. Denton, M. Hesse, M. Kuznetsova, Z. W. Ma, A. Bhattacharjee, A. Otto, et al., J. Geophys. Res. **106**, 3715 (2001).
[21] B. N. Rogers, R. E. Denton, J. F. Drake, and M. A. Shay, Phys. Rev. Lett. **87**, 195004 (2001).
[22] J. F. Drake, M. A. Shay, and M. Swisdak, Phys. Plasmas **15**, 042306 (2008).
[23] N. Bessho and A. Bhattacharjee, Phys. Rev. Lett. **95**, 245001 (2005).
[24] W. Daughton and H. Karimabadi, Phys. Plasmas **14**, 072303 (2007).
[25] M. Swisdak, Yi-Hsin Liu, and J. F. Drake, Astrophys. J. **680**, 999 (2008).
[26] Yi-Hsin Liu, W. Daughton, H. Karimabadi, H. Li, and S. P. Gary, Phys. Plasmas **21**, 022113 (2014).
[27] J. M. TenBarge, W. Daughton, H. Karimabadi, G. G. Howes, and W. Dorland, Phys. Plasmas **21**, 020708 (2014).
[28] A. Stanier, A. N. Simakov, L. Chacoń, and W. Daughton, Phys. Plasmas **22**, 010701 (2015).
[29] P. A. Cassak, R. N. Baylor, R. L. Fermo, M. T. Beidler, M. A. Shay, M. Swisdak, J. F. Drake, and H. Karimabadi, Phys. Plasmas **22**, 020705 (2015).
[30] A. Stanier, A. N. Simakov, L. Chacoń, and W. Daughton, Phys. Plasmas **22**, 101203 (2015).
[31] G. T. Blanchard, L. R. Lyons, O. de la Beaujardière, R. A. Doe, and M. Mendillo, J. Geophys. Res. **101**, 15265 (1996).

[32] S. Wang, L. Kistler, C. G. Mouikis, and S. Petrinec, J. Geophys. Res. **120**, 6386 (2015).

[33] J. Qiu, J. Lee, D. E. Gary, and H. Wang, Ap. J. **565**, 1335 (2002).

[34] J. Lin, Y.-K. Ko, L. Sui, J. C. Raymond, G. A. Stenborg, Y. Jiang, S. Zhao, and S. Mancuso, Ap. J. **622**, 1251 (2005).

[35] H. Isobe, H. Takasaki, and K. Shibata, Ap. J. **632**, 1184 (2005).

[36] M. Ohyama and K. Shibata, Ap. J. **499**, 934 (1998).

[37] T. Yokoyama, K. Akita, T. Morimoto, K. Inoue, and J. Newmark, Ap. J. **546**, L69 (2001).

[38] H. Karimabadi, J. Dorelli, V. Roytershteyn, W. Daughton, and L. Chacón, Phys. Rev. Lett. **107**, 025002 (2011).

[39] A. Stanier, W. Daughton, L. Chacón, H. Karimabadi, J. Ng, Y.-M. Huang, A. Hakim, and A. Bhattacharjee, Phys. Rev. Lett. **115**, 175004 (2015).

[40] J. Ng, Y. Huang, A. Hakim, A. Bhattacharjee, A. Stanier, W. Daughton, L. Wang, and K. Germaschewski, Phys. Plasmas **22**, 112104 (2015).

[41] L. Comisso and A. Bhattacharjee, arXiv:1609.02998 (2016).

[42] M. A. Shay, J. F. Drake, M. Swisdak, and B. N. Rogers, Phys. Plasmas **11**, 2199 (2004).

[43] E. R. Priest and T. G. Forbes, J. Geophys. Res. **91**, 5579 (1986).

[44] P. A. Cassak and J. F. Drake, Phys. Rev. Lett. **707**, L158 (2009).

[45] Yi-Hsin Liu, F. Guo, W. Daughton, H. Li, and M. Hesse, Phys. Rev. Lett. **114**, 095002 (2015).

[46] M. Hesse, S. Zenitani, M. Kuznetsova, and A. Klimas, Phys. Plasmas **16**, 102106 (2009).

[47] M. Hesse and S. Zenitani, Phys. Plasmas **14**, 112102 (2007).

[48] J. Birn, J. E. Borovsky, M. Hesse, and K. Schindler, Phys. Plasmas **17**, 052108 (2010).

[49] J. Sakai and T. Kawata, J. Phy. Soc. Japan **49**, 747 (1980).

[50] L. Sironi, D. Giannios, and M. Petropoulou, arXiv:1605.02071v1 (2016).

[51] F. Guo, Yi-Hsin Liu, W. Daughton, and H. Li, Astrophys. J. **806**, 167 (2015).

[52] N. Bessho and A. Bhattacharjee, Astrophys. J. **750**, 129 (2012).

[53] M. Melzani, R. Walder, D. Folini, C. Winisdoerfer, and J. M. Favre, A & A **570**, A111 (2014).

[54] P. Wu, M. A. Shay, T. D. Phan, M. Oieroset, and M. Oka, Phys. Plasmas **18**, 111204 (2011).

[55] Yi-Hsin Liu, J. F. Drake, and M. Swisdak, Phys. Plasmas **19**, 022110 (2012).

[56] Yi-Hsin Liu, J. F. Drake, and M. Swisdak, Phys. Plasmas **18**, 092102 (2011).

[57] N. F. Loureiro, A. A. Schekochihin, and S. C. Cowley, Phys. Plasmas **14**, 100703 (2007).

[58] W. Daughton, V. Roytershteyn, B. J. Albright, H. Karimabadi, L. Yin, and K. J. Bowers, Phys. Rev. Lett. **103**, 065004 (2009).

[59] Y. M. Huang and A. Bhattacharjee, Phys. Plasmas **17**, 062104 (2010).

[60] L. S. Shepherd and P. A. Cassak, Phys. Rev. Lett. **105**, 015004 (2010).

[61] E. R. Priest and T. R. Forbes, *Magnetic Reconnection* (Cambridge University Press, 2000), chap. 4.2.1, pp. 121–122.

[62] J. Egedal, A. Le, and W. Daughton, Phys. Plasmas **20**, 061201 (2013).

[63] M. Hesse, T. Neukirch, K. Schindler, M. Kuznetsova, and S. Zenitani, Space Sci. Rev. **160**, 3 (2011).